Optical and Quantum Electronics **32:** 619–640, 2000.

Large near resonance third order nonlinearity in GaN

CHI-KUANG SUN[1], YONG-LIANG HUANG[1], JIAN-CHIN LIANG[1], JIUN-CHENG WANG[1], KIAN-GIAP GAN[1], FU-JEN KAO[2], STACIA KELLER[3], MICHAEL P. MACK[3], UMESH MISHRA[3] AND STEVEN P. DENBAARS[3]

[1]*Department of Electrical Engineering and Graduate Institute of Electro-Optical Engineering, National Taiwan University, Taipei 10617, Taiwan, ROC (E-mail: sun@cc.ee.ntu.edu.tw);*

[2]*Department of Physics, National Sun Yat-Sen University, Kaoshiung 80424, Taiwan, ROC;*

[3]*Department of Electrical and Computer Engineering, University of California, Santa Barbara, CA 93106, USA*

Abstract. We have studied third order nonlinearities, including two-photon absorption coefficient β and nonlinear refractive index n_2, of GaN in below bandgap ultraviolet (UV) wavelength regime by using UV femtosecond pulses. Two-photon absorption was investigated by demonstrating femtosecond UV pulse-width autocorrelation in a GaN thin film while femtosecond Z-scan measurements revealed information for both n_2 and β. The distribution of n_2 versus wavelength was found to be consistent with a model described by the quadratic Stark effect, which is the dominant factor contributed to the nonlinear refractive index near the bandgap. Large β on the order of 10 cm/GW and large negative n_2 with a magnitude on the order of several 10^{-12} cm^2/W were obtained. The β at near mid-gap infrared (IR) wavelength was also found to be on the order of several cm/GW by using two-photon-type autocorrelations in a GaN thin film. Taking advantage of the large two-photon absorption at mid-gap wavelengths, we have demonstrated excellent image quality on two-photon confocal microscopy, including two-photon-scanning-photoluminescence imaging and two-photon optical-beam-induced current microscopy, on a GaN Hall measurement sample and an InGaN green light emitting diode.

Key words: GaN, nonlinear refractive index, third-order nonlinearity, two-photon absorption, two-photon confocal microscopy

1. Introduction

Third order nonlinearity plays an important role in optoelectronics. Two-photon absorption (TPA) and nonlinear refractive index effects are among the most frequently encountered third order nonlinearities. Nonlinear refractive index phenomenon, which corresponds to the real part of a $\chi^{(3)}$ process, is widely applied to applications like white light generation, soliton generation, pulse compression, optical switches, optical gating, and miscellaneous optical controls. Two photon absorption, which corresponds to the imaginary part of the $\chi^{(3)}$ process, is also widely applied to pulsewidth measurement and spectroscopic characterizations. For most optoelectronics devices, these two phenomena also play essential roles in determination of the device behaviors. While applications of these nonlinear phenomena have

been widely practiced in visible and IR wavelength regions, their application in ultraviolet (UV) wavelength is limited by available materials. Due to its wide direct bandgap, GaN and its related materials have recently attracted a great deal of interest for their success in light emitters/detectors in the green to UV wavelengths and in high power electronics (Nakamura *et al.* 1996). Motivated by the excellent optical properties of GaN, we have performed studies on the third order nonlinearities, including two-photon absorption and nonlinear refractive index effects, of GaN for below bandgap ultraviolet (UV) wavelength by using UV femtosecond pulses. Huge nonlinearities, for both two-photon absorption and nonlinear refractive index, were observed, indicating GaN also as an excellent nonlinear material for UV applications.

We have also performed two-photon-absorption type autocorrelation measurements at the IR wavelength of above mid-gap energy $E_{\text{gap}/2}$. A large value of β, on the same order but larger than previously reported values (Miragliotta and Wickenden 1996), was obtained. Taking advantage of the large two-photon absorption at above mid-gap IR wavelengths, we have demonstrated two-photon-scanning-photoluminescence imaging and two-photon optical-beam-induced current microscopy on a GaN Hall measurement sample and an InGaN green light emitting diode (LED). Direct correlation was observed between the defect yellow luminescence and the suppression of bandedge photoluminescence. The active region of the green LED was dominated by plalet formation possibly due to the composition inhomogeneity or the strain relaxation between InGaN and GaN layers.

2. Two-photon autocorrelation studies

Recently there are several reports on the studies of the two-photon absorption (TPA) process in GaN. Taking advantage of the TPA process in GaN thin films and photodetectors, autocorrelations and cross-correlations of visible and IR femtosecond pulses have been demonstrated by several research groups (Petit *et al.* 1997; Wada *et al.* 1997; Sun *et al.* 1999; Streltsov *et al.* 1999). Two-photon absorption induced photoluminescence (PL) of GaN was also reported (Kim *et al.* 1997) using tunable picosecond pulses. A large two-photon absorption coefficient β of 17.5 cm/GW at 600 nm wavelength was reported by performing two-photon absorption type autocorrelation in a GaN epilayer (Petit *et al.* 1997). By performing two-photon photocurrent measurements, a large value of $\sim$1.5 cm/GW was also obtained for β at photon energies above $E_{\text{gap}/2}$ in the IR wavelength region (Miragliotta and Wickenden 1996). However, the two-photon absorption coefficients β at UV and blue wavelengths were still unknown. The study of two-photon absorption process for below bandgap UV-blue wavelength is

important due to the fact that most nitride based optoelectronics are operated in this wavelength regime instead of red or infrared wavelength. TPA in this wavelength range will lead to optical power limitation and optical damages in nitride based optoelectronics (Miragliotta and Wickenden 1996). UV two-photon-absorption-type autocorrelation is also important due to the difficulty of finding a suitable second-harmonic generation crystal for wavelength shorter than 400 nm.

In this section, we would like to present our measurement results of two-photon absorption coefficient β at below bandgap UV wavelength by demonstrating two-photon-absorption type UV autocorrelations. Prior to the study in UV wavelength, we have first performed the autocorrelation measurements in a GaN thin film at above $E_{\text{gap}/2}$ IR wavelength. The GaN sample was grown by MOCVD on a double-side polished c-plane sapphire substrate. After annealing the substrate and deposition of a nucleation layer, unintentionally doped GaN layer of 2.5 μm thickness was grown. The crystal structure is wurzite. A room-temperature transmission spectrum indicated that the bandgap of the sample was located at 365 nm. With a bandgap energy around 365 nm, TPA induced band-to-band transition in GaN will allow photons with wavelength up to 730 nm.

The two-photon-absorption type autocorrelation was performed using standard single-color femtosecond transmission pump-probe technique (Petit *et al*. 1997) with a Kerr-Lens-Modelocked Ti:sapphire laser with a repetition rate of 82 MHz. The central wavelength was 720 nm. The laser pulses were split as pump and probe pulses by a beamsplitter. The pump pulses passed through a variable delay stage and were redirected to be parallel to the probe pulses. These two beams were then focused onto the same point on the GaN sample by a thin lens. After the sample, the pump beam and scattered light were rejected using an iris so that only the probe signal will be detected. The pump beam was chopped and the detected probe signal was measured as a function of the temporal delay between the pump and the probe by a lock-in amplifier, so that only the pump-induced probe transmission change was measured. A complimentary transient differential reflection measurement was also performed to remove the transient contribution from surface reflection.

Figure 1 shows a typical measured differential transmission trace of the probe beam as a function of pump-probe delay obtained with a single scan. The measured signal mimics a collinear interferometric autocorrelation trace with interference fringes. However, the data should be treated as an interference pattern superimposed on a background signal. The background signal is the desired transmission autocorrelation trace induced by two-photon absorption process in GaN. The interference pattern is, on the other hand, contributed from the sapphire substrate. To confirm this assumption, the GaN sample was replaced by a comparison sapphire substrate (without

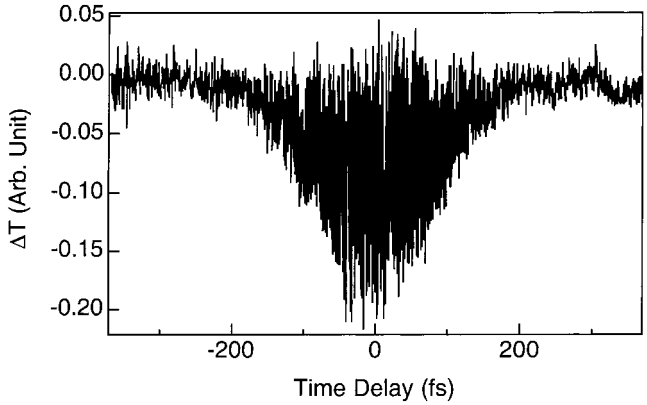

Fig. 1. Single-scan autocorrelation trace for 720 nm IR pulses measured in a GaN thin film with a sapphire substrate.

GaN layer) in the same measurement setup. Figure 2 shows the measured data obtained with a single scan of the repeated measurement on the comparison sapphire substrate. The interference pattern remained but the background signal disappeared. The interference signal might originate from a four-wave-mixing type coherent effect in sapphire. To confirm the detailed physical origin requires further studies. In our measurement, this unwanted interference signal was removed by averaging detected signal through multiple scans, taking advantage of the slight inaccuracy in the repeatability of the delay stage. Figure 3 (open circles) presents a multi-scanned differential probe transmission trace as a function of the probe delay, which is the desired autocorrelation trace with a symmetric pulse shape. The differential transmission change of probe beam decreased linearly with pump excitation power, indicating a two-photon absorption process consisting of one pump

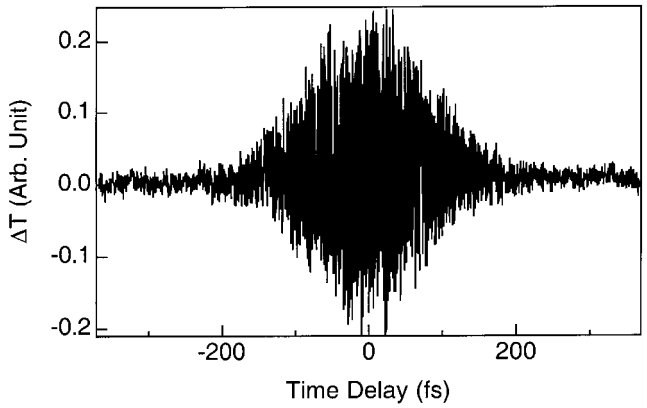

Fig. 2. Single-scan trace for 720 nm IR pulses measured in a comparison sapphire substrate.

photon and one probe photon. The shape of the TPA-induced differential transmission decrease will mimic the pulse autocorrelation function. The pulsewidth can thus be obtained by computer fitting. The dotted line in Fig. 3 shows a fitted Gaussian temporal profile with a full-width-at-half-maximum (FWHM) of 200 fs. With the assumption of a Gaussian profile, a FWHM pulsewidth of ~140 fs can thus be derived for the original pulse. A time-bandwidth product of 0.55 was obtained, combining a spectral FWHM of 6.8 nm measured by an optical multichannel analyzer.

In order to derive the TPA coefficient β, we have calculated the probe transmission decrease due to pump induced absorption assuming Gaussian temporal and spatial profiles with a sample thickness much smaller than the confocal parameter. When the pump and the probe are completely overlapped in both time and space, the maximum differential transmission change $|\Delta T/T|_{\max}$ can be related to the TPA coefficient β through $|\Delta T/T|_{\max} = \beta \cdot l \cdot I_{\text{eff}}$. l is the effective sample thickness and I_{eff} is the effective pump intensity observed by the overlapped probe pulses. However, we have to consider intensity profiles in both time and space domain, which follow Gaussian distributions instead of constants. By integrating the intensity distribution effect in both space and time domains, we can then obtain the following equation,

$$|\Delta T/T|_{\max} \cdot \sqrt{\frac{\pi}{2ln2}} = \beta \cdot l \cdot \frac{E_{\text{p}}}{\tau \cdot \pi \cdot (\frac{R}{2})^2} \tag{1}$$

where E_{p} is the pump pulse energy inside the sample, τ is the FWHM pulsewidth, and R is the $1/e^2$ beam diameter. For the specific trace presented

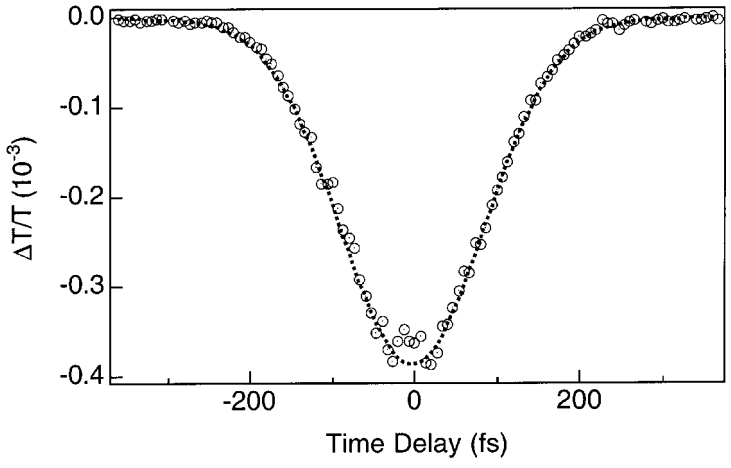

Fig. 3. Multiple-scan autocorrelation trace for 720 nm IR pulses measured by TPA-induced transmission changes in a GaN thin film.

in Fig. 3, the pump pulse energy inside the sample was 240 pJ, corrected after the surface Fresnel reflection. The focal spot diameter R of the IR beam was measured to be 16.3 μm determined by transmission through a 10 μm pinhole. With a sample thickness of 2.5 μm, the maximum probe transmission decrease of 0.04% can thus correspond to a TPA coefficient β of 2.7 ± 1.5 cm/GW at a wavelength of 720 nm. Similar measurements have also been applied to studies of shorter wavelengths. The TPA coefficient β was found to increase with shorter wavelengths. At 690 nm wavelength, a β of 7 ± 3 cm/GW was obtained in a similar measurement procedure. The values of β obtained from our experiments are on the same order but slightly higher than previously reported values, which were on the order of ~1.5 cm/GW, obtained by performing two-photon photocurrent measurements (Miragliotta and Wickenden 1996). However, two-photon transmission measurements usually present better accuracy than two-photon current measurements. The imperfect alignment of the two beams in two-photon transmission measurements, for example partial overlap of the pump-probe in the sample, will only lead to an underestimation of β. The discrepancy might thus be attributed to the possible partial collection of the two-photon currents.

We have then performed our study of the two-photon absorption in GaN for below bandgap ultraviolet (UV) wavelength region. Encouraged by the large TPA coefficient of GaN at longer wavelengths, we believed that GaN and its related materials should be excellent candidate materials for UV pulsewidth measurements using TPA-type techniques. By adding aluminum composition into GaN, the bandgap will be widened and the application wavelength can be further extended into the UV region. The UV two-photon-absorption study was performed in a measurement setup similar to previous IR measurements. The laser output pulses from the femtosecond mode-locked Ti:sapphire laser were frequency-doubled in a 500-μm-thick beta barium borate (BBO) crystal to reach the below bandgap UV wavelength. The frequency-doubled UV femtosecond pulses were tunable between 350 and 400 nm. With 400 mW IR output from the Ti:sapphire laser at a wavelength of 760 nm, the average power of the frequency-doubled UV beam was 30 mW. The UV spatial mode was TEM_{oo}. Having IR pulses been filtered out by a color filter, the UV pulses were then directed into the standard transmission pump-probe setup described previously. A complimentary transient differential reflection measurement was also performed for each transmission measurement to remove the transient contribution from surface reflection.

Figure 4(a) shows the measured probe transient response using UV femtosecond pulses centered at a wavelength of 400 nm (open circles) in a 5 μm-thick GaN sample. Around zero time-delay, a large transmission decrease due to two-photon absorption process was observed. The observed

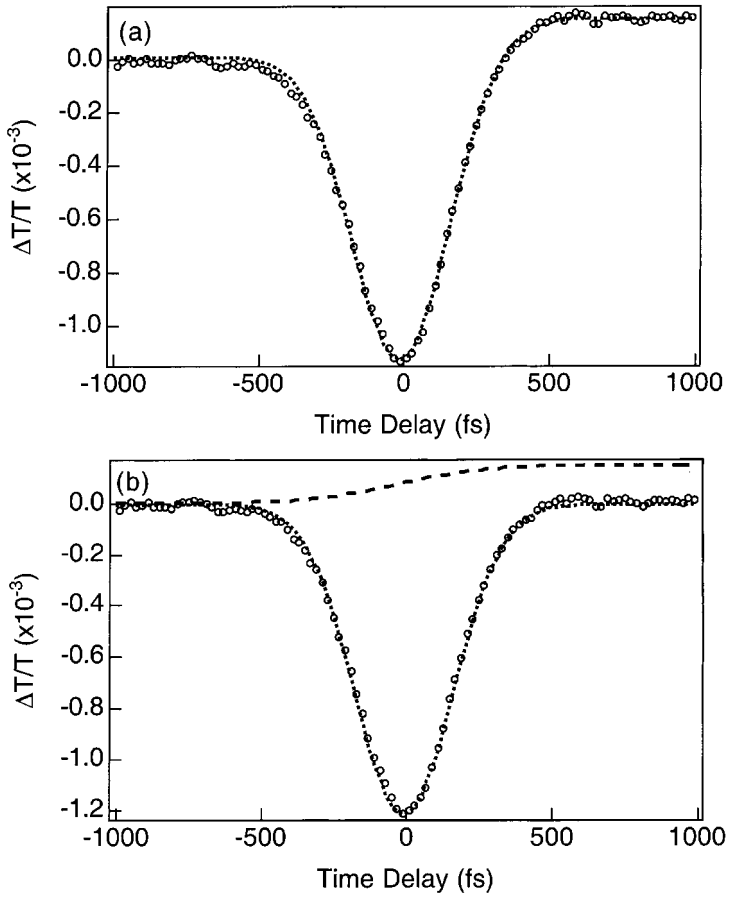

Fig. 4. (a) Transient transmission response (open circles) with 400 nm femtosecond pulses. The dotted line is a convolution fit. (b) The modified data (open circles) after removing the contribution from the convoluted step response (dashed line). The dotted line is a Gaussian fit.

larger TPA transmission decrease indicates a higher value of β at UV wavelengths. The relative magnitude of the sapphire substrate interference signal was much smaller compared with previous IR measurements. Less scans were required to remove the interference effect than IR cases. However, after the TPA decrease, the measured transient response did not return to zero but was followed by a small step-like positive transmission increase within our measured time delay ($\sim$1 ps). This transmission increase should be attributed to the absorption saturation of the bandtail defect states. This bandtail state absorption saturation might be the origin of the non-ideal interferometric autocorrelation pulse shape (a 6:1 ratio instead of an 8:1 ratio) obtained from a GaN p-i-n photodetector using 410 nm femtosecond pulses (Streltsov *et al.* 1999). In order to removed the contribution from the bandtail state absorption saturation, we have performed a convolution fit.

The fitting considers two components: a Gaussian pulseshape (negative, representing the TPA pulsewidth autocorrelation) and its convolution with a step function (positive, representing the contribution from the absorption saturation). The dotted line on top of the experimental data is a convolution fit. The dotted line and the dashed lines in Fig. 4(b) are the corresponding contributions from the negative Gaussian pulseshape and its positive convolution component with a step function. The open circles in Fig. 4(b) are the corrected autocorrelation trace after removing the step function contribution (dashed line in Fig. 4(b)) from the experimental data. An excellent fit with a Gaussian pulseshape was obtained. A temporal FWHM of 400 fs was used in our fitting Gaussian profile. A FWHM pulsewidth of 280 fs with also a temporal Gaussian distribution can thus be derived. The focal spot diameter of the UV beam was measured to be 15.7 μm. For the specific trace presented in Fig. 4, the measured pump pulse energy inside the sample was 190 pJ, corrected after the surface Fresnel reflection. Considering the Gaussian spatial and temporal intensity profiles, a two-photon absorption coefficient of 13 ± 6 cm/GW can thus be derived at a wavelength of 400 nm from the peak transmission decrease of 0.13% following Equation (1). The autocorrelation trace can be measured in our simple experimental setup with a pulse energy as low as 5 pJ.

Similar measurements were also performed at UV wavelengths between 400 nm and 377 nm. Figure 5(a) and (b) shows the measured autocorrelation traces after modification at wavelengths of 390 nm and 380 nm respectively. Values of TPA coefficient β of 16 ± 7 and 12 ± 6 cm/GW were obtained for these specific measured traces. For wavelength shorter than 375 nm, the transient response was found to be dominated by absorption saturation of bandtail states. The fitting procedure we adopted would thus yield greater errors. The measured TPA coefficients of GaN at UV wavelengths are much larger than the reported UV TPA coefficients of diamond (0.75 cm/GW at a wavelength of 310 nm (Dadap *et al.* 1991), 2.3 cm/GW at a wavelength of 282 nm (Reuther *et al.* 1997)) and fused silica (0.045 cm/GW at a wavelength of 267 nm (Streltsov *et al.* 1998)), which have both been proposed as candidate two-photon absorption materials for UV pulsewidth autocorrelation. The measured and thus obtained large two-photon absorption coefficients of GaN indicate great potential of nitride-based III-V materials as nonlinear crystals for visible-UV photonic applications. Even though the applicable wavelength was limited by the bandgap of GaN at a wavelength of 365 nm, it can be easily extended further into UV wavelength range by adding aluminum composition into GaN or into IR wavelength by adding indium composition into GaN.

Figure 6 summarizes the measured results. Open circles represent the values obtained from TPA autocorrelation measurements, while open triangles represent the values from Z-scan measurements (see Section III).

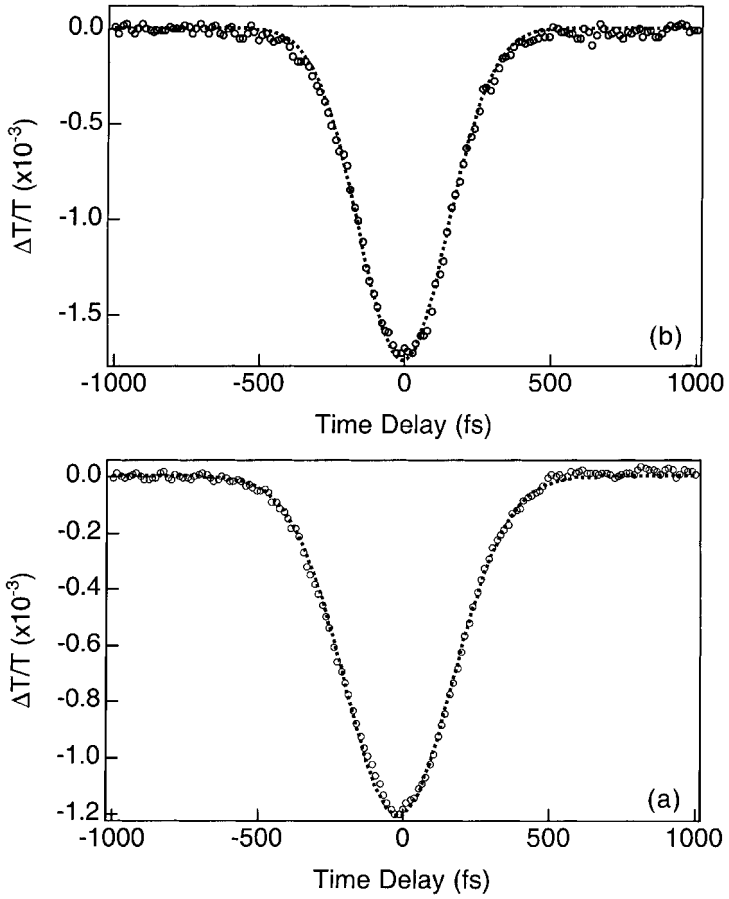

Fig. 5. (a) Measured TPA autocorrelation trace after modification at 390 nm wavelength. (b) Measured TPA autocorrelation trace after modification at 380 nm wavelength.

Previously reported value (Petit *et al.* 1997) at 600 nm is also displayed as a solid diamond for reference. According to the study of Sheik-Bahae and his coworkers, TPA coefficient β of a direct bandgap semiconductor at a photon energy hv can be described by (Sheik-Bahae *et al.* 1991).

$$\beta(hv) = K\frac{\sqrt{E_p}}{n_0^2 E_g^3} F_2\left(\frac{hv}{E_p}\right) \tag{2}$$

with $F_2(x) = (2x-1)^{1.5}/(2x)^5$. K is 1940 while β is in unit of cm/GW. E_p is $\sim$21 eV. E_g is the bandgap energy of GaN of 3.39 eV. n_0 is the refractive index of GaN with (Yu *et al.* 1997)

$$n_0^2 = 5.15 + \frac{0.093}{\lambda^2 - 0.0864}, \tag{3}$$

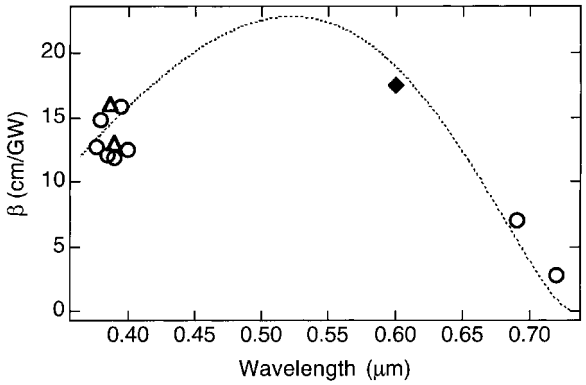

Fig. 6. Measured TPA coefficient versus wavelength. Open circles represent the values obtained from TPA autocorrelation measurements. Open triangles represent the values obtained from Z-scan measurements. Previously reported value from Petit *et al.* (1997) is also displayed as a solid diamond for comparison. Dotted line is 12 times of Equation (2).

while wavelength λ is in unit of μm. We plot 12 times of Equation (2) as a dotted line in Fig. 6 for comparison. Our measured results agree well with the frequency dependence described by Equation (2) but are larger by a constant (12 for this specific case), which is commonly observed in wide-bandgap dielectrics (Sheik-Bahae *et al.* 1991).

3. Z-Scan studies

Since GaN showed its excellent third order nonlinearity through two-photon absorption for below bandgap UV wavelengths, we were thus encouraged to study its nonlinear refractive index property in this wavelength region. An exceptional large positive nonlinear refractive index n_2 of 1×10^{-12} cm^2/W at a wavelength of 532 nm has been previously reported (Taheri *et al.* 1996) by using pulsed probe degenerate four-wave-mixing experiments.

We performed our nonlinear refractive index studies by using Z-scan techniques (Sheik-Bahae *et al.* 1990). Among all techniques for nonlinear refractive index measurement, Z-scan is the most popular method due to its simple experimental setup and easy alignment. However, this technique requires large nonlinear refractive index, high quality TEM_{oo} Gaussian mode laser beams, and smooth and uniform samples. The experiments were performed using the frequency-doubled UV pulses from the femtosecond mode-locked Ti:sapphire. The UV pulsewidth can be obtained through previous TPA-type autocorrelations. The spectral FWHM of the frequency-doubled pulses ranged between 2.5 to 3 nm. The experiments were performed using a standard Z-scan technique with a 25 mm focal length objective. The incident pulse energies at the front sample surface corrected for Fresnel reflection was

between 0.18 nJ and 0.32 nJ. As the 5 μm-thickness GaN sample moved through the focus in the beam propagation direction (called 'Z' direction), the far field transmittance through a finite aperture was measured by a slow photodetector. With self-focusing or self-defocusing effects induced by nonlinear refractive index due to a Gaussian-shaped spatial intensity profile, a Z-scan trace with a peak and a valley could thus be obtained. The value of n_2 could then be evaluated from the peak-to-valley difference of the measured trace (Sheik-Bahae *et al.* 1990).

Surface roughness, wedge, contamination, defects, and sample non-uniformity will cause light scattering or beam pointing variation, which would lead to variations in background transmission during Z-scans and would mask the signals induced by nonlinear refractive index. A low energy scan was used to establish a background reference signal. The parasitic effect can then be removed by subtracting the low-energy reference trace from a high energy trace (Sheik-Bahae *et al.* 1990). In order to remove possible contribution from the sapphire substrate, we have also repeated our measurements on a comparison sapphire substrate. No signal was found. A typical small aperture Z-scan trace and open aperture background signal measured at a wavelength of 371 nm are shown as open circles in Fig. 7(a) and (b) with a small aperture transmittance S (Sheik-Bahae *et al.* 1990) equal to 80%. The dotted lines on top of the measured signals are fitting curves with a beam diameter of 10 μm. Even though a recent report confirmed the accuracy of spot size determination by using open aperture Z-scan traces combined with a fitting procedure (Loka and Smith 1999), we have performed spot size measurement using a pin hole. Excellent agreements were obtained. The measured trace shows a negative sign for n_2. The peak was found to be enhanced and the valley was found to be suppressed. This behavior was an indication of absorption saturation for higher optical intensity close to the beam waist. This behavior was also reflected in the open aperture trace shown in Fig. 7(b). With a saturable absorption coefficient $\alpha(I)$ of the form

$$\alpha(I) = \frac{\alpha_0}{1 + I/I_s}, \tag{4}$$

$\alpha(I)$ can be expanded into

$$\alpha(I) \cong \alpha_0 - (\alpha_0/I_s)I \tag{5}$$

for $I/I_s \ll 1$. α_0 is the linear absorption coefficient, I is the irradiance, and I_s is the saturation irradiance. Compared with the absorption with TPA coefficient β,

$$\alpha(I) = \alpha_0 + \beta I, \tag{6}$$

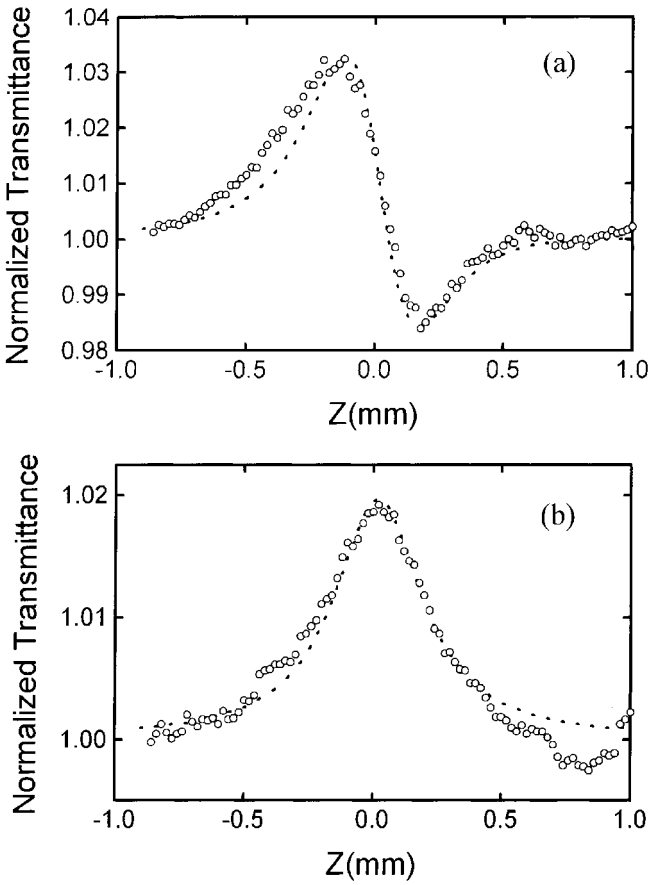

Fig. 7. (a) Small aperture Z-scan trace of GaN measured at 371 nm. The dotted line is a fitting curve with a beam diameter of 10 μm. (b) Open aperture background signal at 371 nm and its fitting curve.

absorption saturation thus functions as an effective negative two-photon absorption coefficient β_{eff} with (Sheik-Bahae *et al.* 1990; Rangel-Rojo *et al.* 1998)

$$\beta_{\text{eff}} \cong -\alpha_0/I_s. \tag{7}$$

A similar behavior was previously reported in an azobenzene-functionalized polymer film (Rangel-Rojo *et al.* 1998). We attribute our observed effect to the absorption saturation of bandtail defect states in the measured GaN sample. With $\alpha_0 = \sigma\rho$ (Koechner 1996), where σ is the absorption cross-section of the defect states and ρ is the defect density of states, and $I_s = h\nu/\sigma\tau_f$, where τ_f is the defect state lifetime, we can then obtain

$$|\beta_{\text{eff}}| \propto \rho. \tag{8}$$

The measured β_{eff} thus reflects the defect state distribution. Following the standard deviation procedure provided by Sheik-Bahae *et al.*, an n_2 of -1.4×10^{-12} cm^2/W and a β_{eff} of -37 cm/GW could thus be derived from this specific Z-scan measurement with a measured pulse energy of 210 pJ and a FWHM pulsewidth of 180 fs.

Z-scan measurements were also performed at different wavelengths between 368 and 391 nm or at different sample position. As we tuned the laser toward shorter wavelength, stronger saturation absorption behavior was observed. The magnitude of nonlinear refractive index was also found to be larger. A small aperture Z-scan trace and its open aperture background signal measured at a wavelength of 369 nm are shown in Fig. 8(a) and (b). The dotted lines are fitting curves with a beam diameter of 10 μm. An n_2 of -2.2×10^{-12} cm^2/W and a β_{eff} of -92 cm/GW could be derived from these

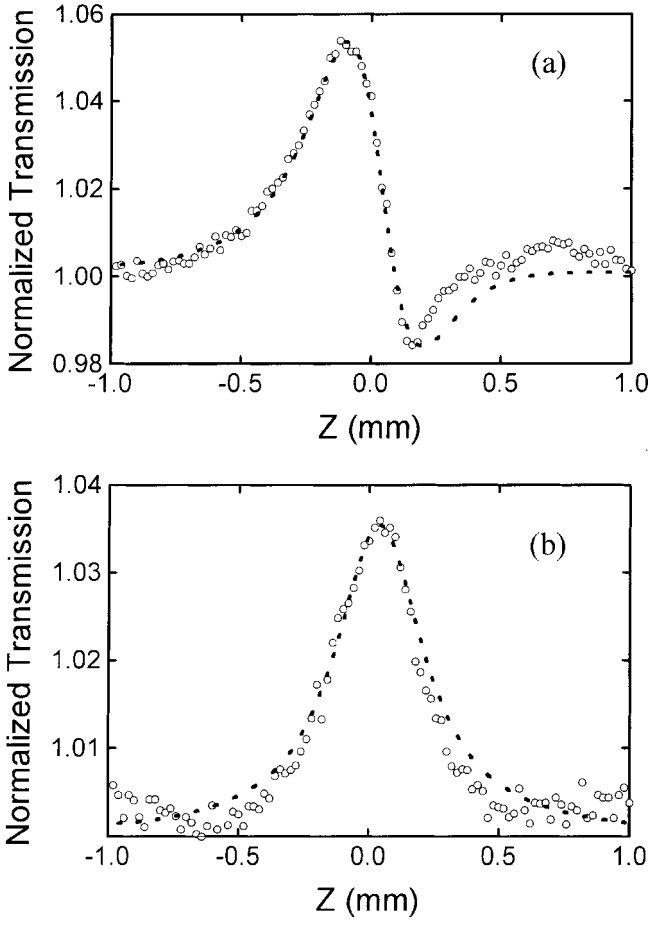

Fig. 8. (a) Small aperture Z-scan trace of GaN measured at 369 nm. The dotted line is a fitting curve with a beam diameter of 10 μm. (b) Open aperture background signal at 369 nm and its fitting curve.

specific Z-scan traces. As we tuned our laser toward longer wavelength, this absorption saturation behavior gradually disappeared. Figure 9 shows the measured β_{eff} distribution versus wavelength. A fitting using an exponential decay of 20 meV is shown as a dashed line in Fig. 9 for reference. Our measurements indicate that the defect bandtail states in this particular sample is mainly distributed within 80 meV below the bandgap. This measurement results agree well with the pump-probe measurements presented in Section II where the transient responses were found to be dominated by absorption saturation of bandtail states for wavelength shorter than 375 nm.

As we tuned our laser toward longer wavelength, the measured small aperture Z-scan traces first became symmetric, then the peak was found to be suppressed and the valley was found to be enhanced, an indication of the two-photon absorption effect. Figure 10 shows a measured small aperture Z-scan trace at a wavelength of 375 nm while Fig. 11 shows a measured small aperture Z-scan trace at a wavelength of 387 nm. The dotted lines in Figs. 10 and 11 are fitting curves. A symmetric Z-scan trace was observed for the 375 nm measurement while the two-photon absorption effect is reflected in the 387 nm trace, indicating the domination of the two-photon absorption effect over the bandtail absorption saturation for longer wavelengths. TPA coefficients of 17 ± 7 and 14 ± 6 cm/GW can be derived from Z-scan traces for wavelengths of 387 and 391 nm, respectively. These measured values are presented in Fig. 6 as open triangles and excellent agreements with previous autocorrelation measurements can be observed.

The measured nonlinear refractive index versus wavelength is summarized in Fig. 12 (open circles). n_2 values of $-2.9 \pm 1.2 \times 10^{-12}$, $-1.2 \pm 0.5 \times 10^{-12}$, and $-0.5 \pm 0.2 \times 10^{-12}$ cm^2/W can be obtained for wavelengths of

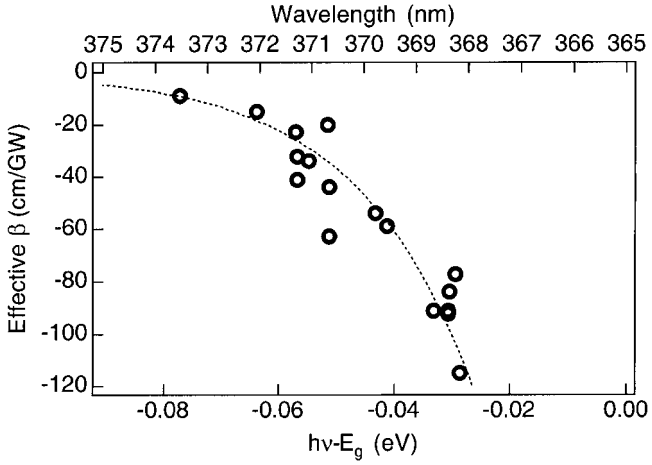

Fig. 9. Measured effective TPA coefficient β_{eff} due to absorption saturation (open circles) versus wavelength. The dotted line is an exponential fit with a decay constant of 20 meV.

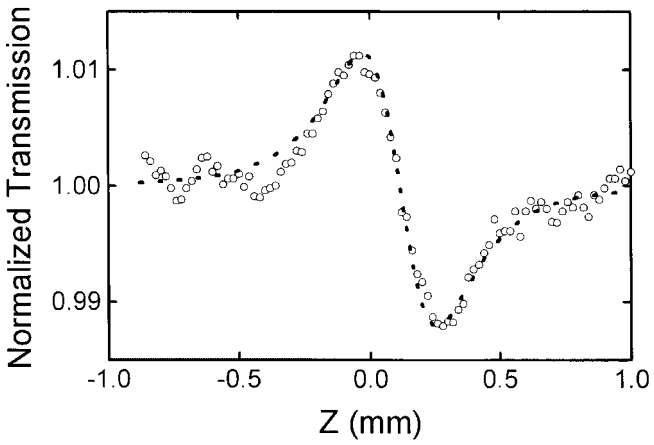

Fig. 10. Small aperture Z-scan trace of GaN measured at 375 nm. The dotted line is a fitting curve.

368, 371, and 380 nm, respectively. Sheik-Bahae *et al.* have derived a formula (Sheik-Bahae *et al.* 1991) for frequency dependent n_2 by a two-parabolic band model based on the Kramer-Krönig relationship. The scaled form for n_2 is given by (Sheik-Bahae *et al.* 1991)

$$n_2(\text{esu}) = K' \frac{\sqrt{E_p}}{n_0 E_g^4} G_2\left(\frac{h\nu}{E_g}\right) \tag{9}$$

where the function G_2 contains the band-structure dependent information. The value of K' predicted by the theory gives 0.94×10^{-8} when E_p and E_g are defined in eV. Previous study showed that the most significant contribution

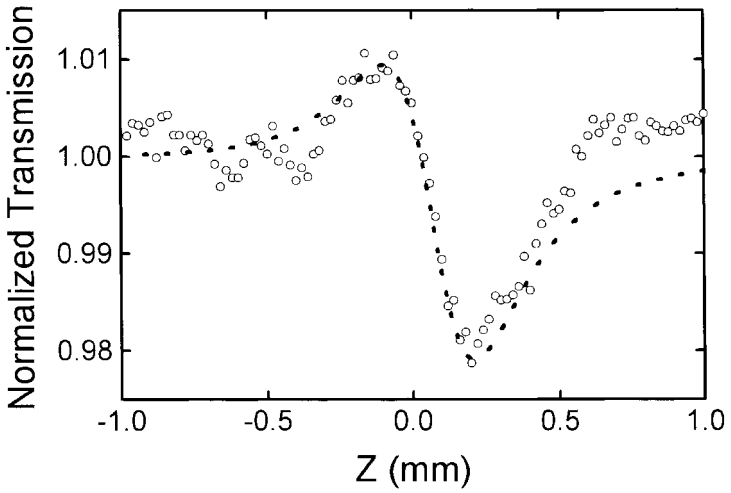

Fig. 11. Small aperture Z-scan trace of GaN measured at 387 nm. The dotted line is a fitting curve.

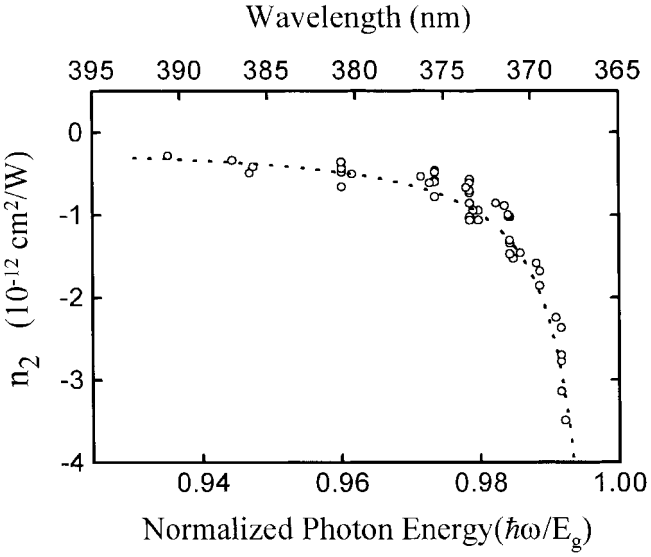

Fig. 12. Measured nonlinear refractive index (open circles) versus wavelength. The dotted line is a reference curve governed by quadratic Stark and two-photon absorption effects.

to the spectral dependence of G_2 arised from the two-photon absorption term, except close to the bandedge where the quadratic Stark term became dominant. The functions G_2 of these two processes can be found in Sheik-Bahae *et al.* (1991). Previous results also indicated that the quantitative agreement of the theory with experiments for wide bandgap materials is not well, although the general trends describing the frequency dependence can be followed (Sheik-Bahae *et al.* 1991). A reference curve (dotted line) following Equation (9) with 12 times of the TPA contribution and 20 times of the quadratic Stark contribution is shown in Fig. 12. An excellent agreement can be obtained, indicating the quadratic Stark effect and the two-photon absorption process as the dominant contributions to the nonlinear refractive index near the bandedge of GaN. When the optical photon energy is close to the bandgap energy, the magnitude of the nonlinear refractive index will increase greatly due to the quadratic Stark effect. The magnitude of n_2 of GaN obtained from our measurements are on the same order with the positive n_2 previously reported at 532 nm (Taheri *et al.* 1996) and the negative n_2 reported at close resonance below bandgap IR wavelengths in AlGaAs (LaGasse *et al.* 1990).

Large nonlinear refractive indexes are seldom reported in UV wavelength region. SiO_2 has been reported to have a positive n_2 of 4.45×10^{-16} cm^2/W (1.7×10^{-13} esu) at 249 nm (Ross *et al.* 1990). Values of 0.69×10^{-16} cm^2/W for MgF_2 and 7.68×10^{-16} cm^2/W for Al_2O_3 were previously reported at 355 nm wavelength (Sheik-Bahae *et al.* 1992). Comparing our measured n_2 of

GaN with these data, the close resonance n_2 of GaN in UV wavelength is 10^3–10^4 order larger than those previously reported values from other UV materials. Our studies indicate that GaN is not only an excellent light emitting material, but also an excellent nonlinear material with a large negative n_2 for UV light controls. Combined with the larger positive group velocity dispersion of GaN at the near UV wavelength, this large negative n_2 of GaN in this wavelength region also indicates GaN as an excellent material system for UV soliton generation. This large negative n_2 of GaN might be responsible for the short optical pulse generation observed in InGaN/GaN laser diodes.

4. Two-photon confocal microscopy

Taking advantage of the large two-photon absorption coefficient of GaN at midgap IR wavelength, the two-photon confocal scanning microscopy on GaN can be easily demonstrated using femtosecond IR pulses. Confocal laser scanning microscopy provides a significant improvement in axial resolution over conventional epi-fluorescence microscopy by eliminating out-of-focus fluorescence using a spatial filter in the form of a confocal aperture (White *et al*. 1987). Combining two-photon induced fluorescence with laser scanning microscopy, Denk *et al*. (1990) achieved high axial/depth discrimination even without a confocal aperture in front of the photodetector, due to the quadratic dependence of the two-photon absorption on the laser intensity. Strong fluorescence is only induced in the vicinity of the focal point. The background scattering light and autofluorescence of the sample in the two-photon-excited system is also lower. The use of infrared wavelength leads to a deeper penetration depth in most materials, providing an opportunity to image thicker samples. For GaN studies, the use of IR excitation wavelength can also avoid most expensive UV lens and mirrors.

Our experiments were performed with an inverted microscope and a galvano-mirror based scanning system. The Kerr-lens-modelocked Ti:sapphire laser provided IR laser pulses of 140 fs tunable between 700–800 nm for two-photon excitation, which is equivalent to 350–400 nm single-photon excitation wavelength. Femtosecond IR pulses passed through XY galvano-mirrors to perform two-dimensional scanning. The dithered laser beam was then directed into an inverted optical microscope (Olympus BX50). An objective was employed to focus the laser beam onto the GaN layer. The average power incident on the GaN samples was between 5 to 10 mW. The valence band carriers were photoexcited into conduction band by strong two-photon absorption and the subsequent photoluminescence (PL) was collected by the same microscope objective, separated from the input laser beam by a long-wavelength pass beamsplitter, and directed into a photomultiplier (PMT) tube. Band-pass filters were used to select specific spectral band for PL im-

ages. Due to the large wavelength difference between the IR excitation pulse and the PL light, the luminescent photons can be easily separated from the pump laser beam. Combined with the strong two-photon absorption in GaN, large signal-to-noise ratio can thus be easily achieved. Also due to the IR excitation wavelength, no UV optics were required in the excitation set-up, except for the necessary PL measurements.

We have also performed two-photon optical beam induced current (OBIC) imaging in an InGaN green LED. With below bandgap two-photon excitation, OBIC (Xu and Denk 1997) can be performed with reduced absorption and reduced scattering in the overlayers of a device. Combined with the large TPA coefficient of GaN, excellent depth resolution can thus be easily achieved. For two-photon OBIC imaging, the samples under test were connected to a current amplifier for TPA-induced photocurrent (PC) measurements.

Figure 13(a) and (b) show the measured two-photon scanning PL images of a GaN Hall-measurement sample. The excitation wavelength was 720 nm. Excellent image quality can be observed. Figure 13(a) is an image taken with a 365-nm interference filter with a 10-nm bandwidth in front of the PMT tube, corresponding to the GaN band-to-band transitions at room temperature. Figure 13(b) is an image taken with a 550–650 nm bandpass filter, corresponding to the wavelength of the below-bandgap yellow luminescence. Figure 13(c) shows an image taken with the transmitted 720-nm light through the sample. The image was taken from the edge of the Hall measurement sample with two oval defects. Figure 13(a) indicates excellent lateral uniformity in the measured sample except on the areas around oval defects. It's interesting to notice that the area emitting weak bandedge luminescence corresponds to the area emitting strong yellow luminescence. The yellow photoluminescence of GaN has been thought to compete with the edge photoluminescence and was studied intensively recently (Godlewski *et al.* 1998). Our demonstration indicates that two-photon confocal microscopy should be an excellent tool for detailed investigations.

Figures 14(a) and (b) show two-photon PL and two-photon OBIC images of a commercially available green LED dice. The IR laser beam was focused through the sapphire substrate at the InGaN active layer at a wavelength of 760 nm to avoid possible two-photon excitation in n-doped and p-doped GaN layers. The PL image was taken with a green bandpass filter while a high-sensitive current amplifier was used to detect the PC in the two-photon OBIC image. The most pronounced features in the PL and PC images are the bright spots covering all over the LED. These spots have the sizes ranging from 5 μm to less than the resolution of the objective, which is on the order of 1.3 μm. The locations of the bright spots on PL and PC images show strong correlation, indicating the same physical origin. Similar bright spots were also observed in electro-luminescence images. Since we have avoided any excitation in the GaN layers, these bright spots should not originate from

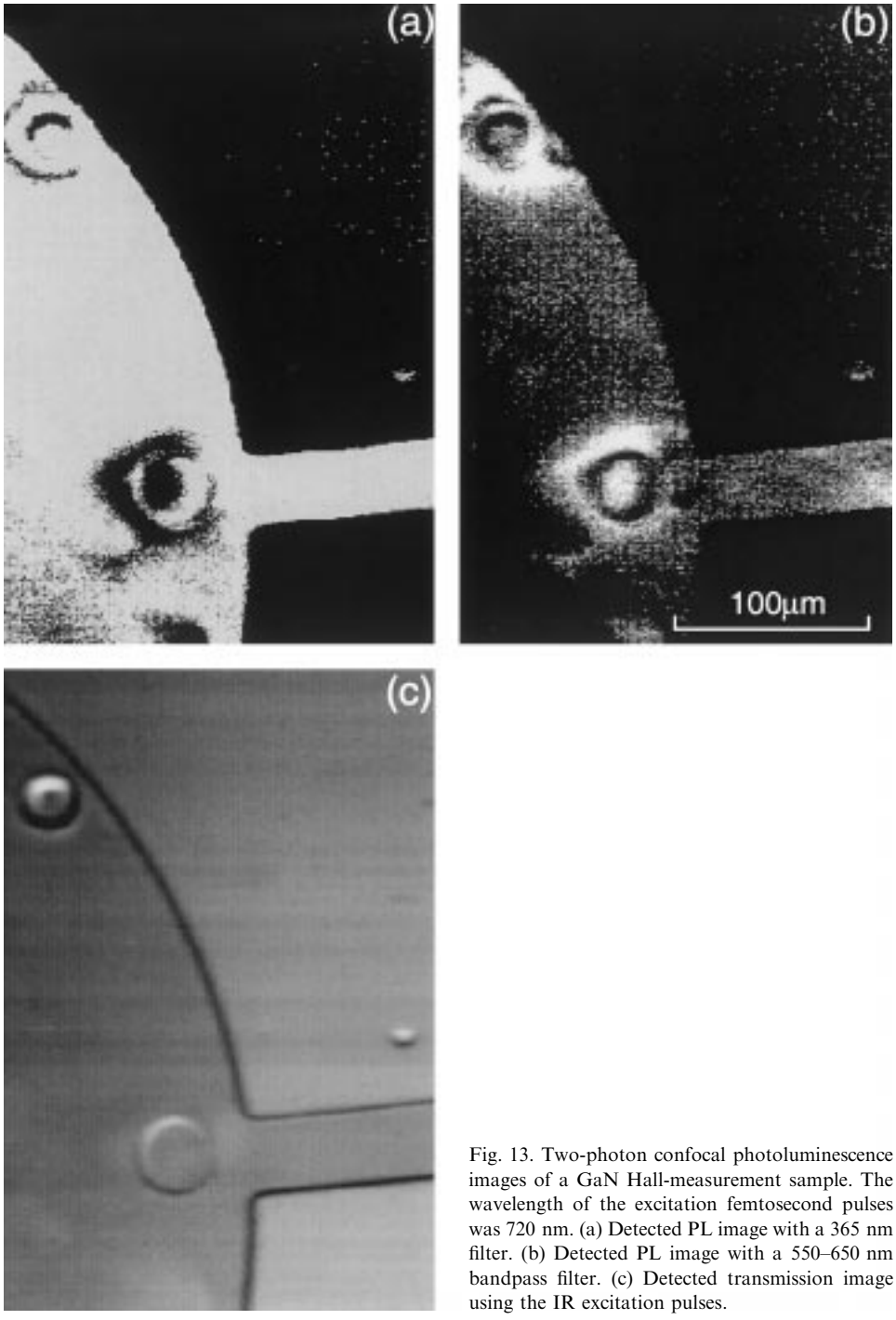

Fig. 13. Two-photon confocal photoluminescence images of a GaN Hall-measurement sample. The wavelength of the excitation femtosecond pulses was 720 nm. (a) Detected PL image with a 365 nm filter. (b) Detected PL image with a 550–650 nm bandpass filter. (c) Detected transmission image using the IR excitation pulses.

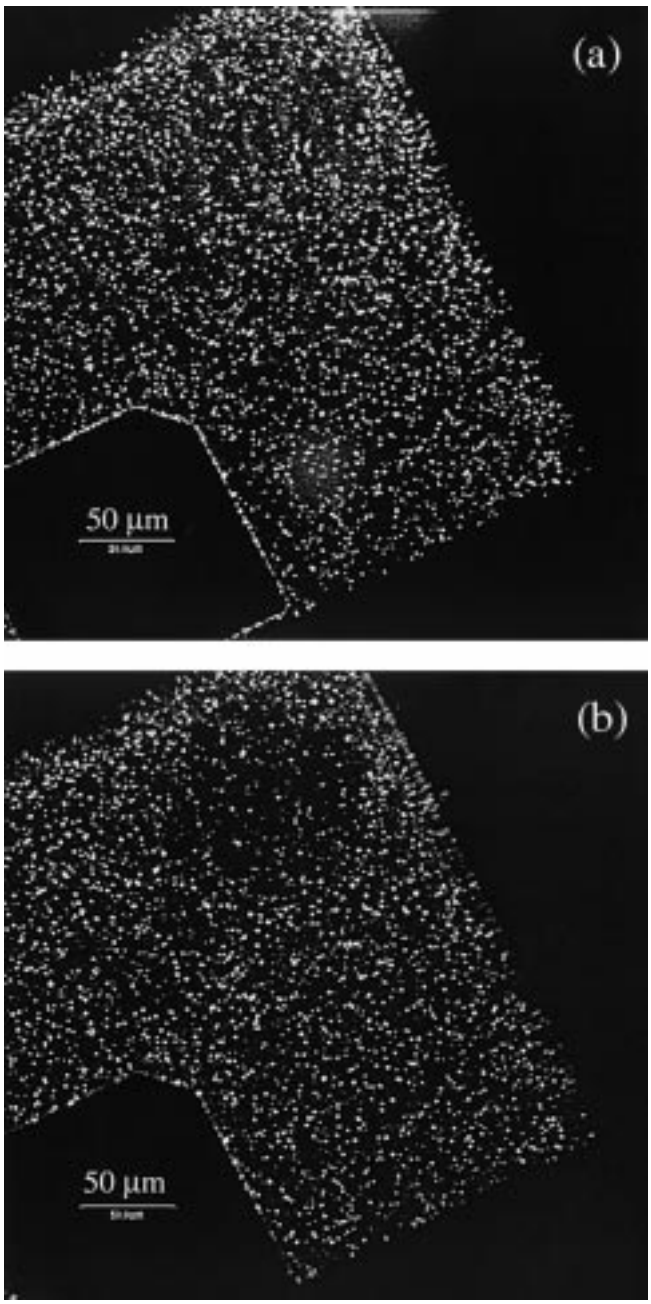

Fig. 14. (a) Two-photon PL image and (b) two-photon OBIC image of a green InGaN/GaN LED. The excitation wavelength was 760 nm. A green filter was used in the PL image.

the p-doped GaN layer. Possible mechanisms include InGaN plalet formation due to the strain relaxation between InGaN and GaN layers or due to composition inhomogeneity. Our demonstration indicates that with the two-photon excitation technique, which is much less susceptible to scattering and absorption, nitride-based optoelectronic devices with multilayered heterostructure can be easily imaged and studied without much sample preparation. We have also performed single-photon confocal PL & PC images. Two-photon excitation clearly exhibits better spatial resolution and reveals more interesting features not observed before.

5. Summary

In summary, large near resonance third order nonlinearities, including two-photon absorption and nonlinear refractive index, of GaN were observed. We studied two-photon absorption of GaN by demonstrating two-photon absorption autocorrelation measurements while the nonlinear refractive index was investigated using Z-scan techniques. At below bandgap UV wavelengths, two-photon absorption coefficient was found to be on the order of 10 cm/GW while nonlinear refractive index was found to be on the order of -1×10^{-12} cm^2/W. These large UV nonlinearities indicate GaN and it related materials as excellent candidates for UV nonlinear applications.

Large two-photon absorption coefficients at above midgap IR wavelength were also observed. Taking advantages of the large two-photon absorption coefficients at above midgap IR wavelength, we have demonstrated two-photon confocal scanning microscopy, including photoluminescence images and photocurrent images, on a GaN Hall measurement sample and an InGaN green LED using infrared femtosecond pulses. With two-photon excitation technique that is much less susceptible to scattering and absorption, GaN based devices with multilayered heterostructure can thus be easily imaged and studied. Two-photon excitation study of GaN clearly exhibits better spatial resolution and reveals interesting features not observed before. Direct correlation was observed between the defect yellow luminescence and the suppression of bandedge photoluminescence. The active region of the green LED was found to be dominated by plalet formation possibly due to the composition imhomogeneity or the strain relaxation between InGaN and GaN layers.

Acknowledgement

This project is sponsored by National Science Council of Taiwan, ROC under grant number NSC 88-2112-M-002-003.

References

Dadap, J.I., G.B. Focht, D.H. Reitze and M.C. Downer. *Opt. Lett.* **16** 499, 1991.
Denk, W., J.H. Strickler and W.W. Webb. *Science* **248** 73, 1990.
Godlewski, M., E.M. Goldys, M.R. Phillips, R. Langer and A. Barski. *Appl. Phys. Lett.* **73** 3686, 1998.
Kim, D., I.H. Libon, C. Voelkmann, Y.R. Shen and V. Petrva-Koch. *Phys. Rev. B* **55** 4907, 1997.
Koechner, W. *Solid State Laser Engineering*, 4th ed, Springer-Verlag, Berlin, 1996.
LaGasse, M.J., K.K. Anderson, C.A. Wang, H.A. Haus and J.G. Fujimoto. *Appl. Phys. Lett.* **37** 555, 1990.
Loka H.S. and P.W.E. Smith. *Optics and Photonics News* **10**, engineering and laboratory notes, 1999.
Miragliotta, J. and D.K. Wickenden. *Appl. Phys. Lett.* **69** 2095, 1996.
Nakamura, S., M. Senoh, N. Iwasa, T. Yamada, T. Matsushita, H. Kiyoku and Y. Sugimoto. *Jpn. J. Appl. Phys.* **35** L74, 1996.
Petit, S., D. Guennani, P. Gilliot, C. Hirlimann, B. Hönerlage, O. Briot and R.L. Aulombard. *Materials Science and Engineering B* **43** 196, 1997.
Rangel-Rojo, R., S. Yamada, H. Matsuda and D. Yankelevich. *Appl. Phys. Lett.* **72** 1021, 1998.
Reuther, A., A. Laubereau and D.N. Nikogosyan. *Optics Communication* **141** 180, 1997.
Ross, I.N., W.T. Toner, C.J. Hooker, J.R.M. Barr and I. Coffey. *J. Modern Opt.* **37** 555, 1990.
Sheik-Bahae, M., J.R. DeSalvo, A.A. Said, D.H. Hagan and E.W. Van Stryland. *Proc. SPIE* **1624** 25, 1992.
Sheik-Bahae, M., D.C. Hutchings, D.J. Hagan and E.W. Van Stryland. *IEEE J. Quantum Electron.* **27** 1296, 1991.
Sheik-Bahae, M., A.A. Said, T.H. Wei, D.J. Hagan, E.W. Van Stryland. *IEEE J. Quan. Elec.* **26** 760, 1990.
Streltsov, A.M., A.L. Gaeta, P. Kung, D. Walker, M. Razeghi. In *Technical Digest of Conference on Laser and Electro-optics*, Baltimore, MD, paper CFG6, 1999.
Streltsov, A.M., J.K. Ranka and A.L. Gaeta. *Opt. Lett.* **23** 798, 1998.
Sun, C.-K., Y.-L. Huang, J.-C. Wang, S. Keller, M. Mack, U.K. Mishra and S.P. DenBaars. In *Technical Digest of Conference on Laser and Electro-optics*, Baltimore, MD, paper CTuI4, 1999.
Taheri, T., J. Hays, J.J. Song and B. Goldenberg. *Appl. Phys. Lett.* **68** 587, 1996.
Wada, A., W. Ho and M.A. Khan. *Thin Solid Films* **306** 137, 1997.
White, J.C., W.B. Amos and M. Fordham. *J. Cell Biology* **105** 41, 1987.
Xu C. and W. Denk. *Appl. Phys. Lett.* **71** 2578, 1997.
Yu, G., G. Wang, H. Ishikawa, M. Umeno, T. Soga, T. Egawa, J. Watanabe and T. Jimbo. *Appl. Phys. Lett.* **70** 3209, 1997.